Iron Doped Nanosheet-Assembled Ni₃(NO₃)₂(OH)₄ Spheres with Enhanced Photocatalytic Properties

WEIWEI WANG*, YINGWEI XU, AIJUAN ZHANG and CHENGFENG LI

School of Materials Science and Engineering, Shandong University of Technology, 12 Zhang Zhou Road, Zibo 255091, Shandong, P.R. China

*Corresponding author: Fax: +86 533 2781660; Tel: +86 533 2782198; E-mail: weiweiwangsd@aliyun.com

Iron ions play a critical, but yet unclear, role in improving the activity of Ni-based catalysts. To investigate the changes of iron ions doping in photocatalytic properties, we prepared undoped and Fe doped nanosheet-assembled $Ni_3(NO_3)_2(OH)_4$ spheres and particles by a simple hydrothermal method, which used urea to provide OH⁻. The effects of the iron ions and urea on the preparation of the $Ni_3(NO_3)_2(OH)_4$ structures were explored. In the presence of Fe, low concentration of urea favors the formation of $Ni_3(NO_3)_2(OH)_4$ particles, while high concentration prefers the formation of well-crystallized nanosheet-assembled $Ni_3(NO_3)_2(OH)_4$ spheres. Without Fe doping, only nanosheet-assembled $Ni_3(NO_3)_2(OH)_4$ spheres were obtained and more urea resulted in the formation of poor-crystallized $Ni_3(NO_3)_2(OH)_4$ spheres. Fe doped nanosheet-assembled $Ni_3(NO_3)_2(OH)_4$ spheres and particles with holes on the surface exhibited good photocatalytic activity in the degradation of methyl orange.

Keywords: Layered compounds, Doping, Hierarchical sphere, Photocatalytic property.

INTRODUCTION

Nickel based catalysts including Ni, Ni_2O_3, $Ni(OH)_2$ and NiOOH, have attracted increasing attention from researchers worldwide because it is low cost and more active compared with noble and other transition metals[1-3]. For applications in the elimination of organic pollutions, those Ni species had mainly been used by loading on the surface of other materials. For example, with loading Ni species on the surface of SnO_2 nanoparticles, Ni_2O_3 could suppress the recombination of photogenerated electrons and holes while $Ni(OH)_2$ could enhance light absorption of SnO_2[4]. Loading $Ni(OH)_2$ clusters on the surface of TiO_2 significantly enhanced its photocatalytic hydrogen production activity[5]. Doping with Ni in RVO_4 (R = Y, Gd) contributes to the electron carriers separation, thus enhancing H_2 generation[6]. Those Ni species in catalysts could promote direct electron transfer reactions or improve the photoinduced charge transfer of catalysts[4,7].

Among those Ni species, nickel hydroxide nitrate [$Ni_3(NO_3)_2(OH)_4$], as a typical representative of layered hydroxide salts, shows a similar structure to that of brucite, where one-fourth of the OH⁻ groups are substituted by nitrate ligands in an ordered way. $Ni_3(NO_3)_2(OH)_4$ with a layered structure shows large surface areas, ion exchange properties and intercalation capacities. These properties, along with the function of Ni species as catalysts, make them appealing for use in waste water treatment. Recent advances have shown that $Ni_3(NO_3)_2(OH)_4$ could be used as a typical active material for electrochemical capacitors or a precursor for the preparation of NiO[8,9], while such studies are few for the application in waste water treatment. In addition, it has further shown that iron ions can affect the electronic structure of NiOOH which also adopts a brucite structure by inducing partial-charge transfer[10]. The brucite-structured layered double hydroxides (LDHs) with both Ni and Fe have the highest activity in the water oxidation reaction because the presence of Fe and Ni can improve the diffusion of reactants and products[11]. Despite these studies that indicated that iron ions are useful in enhancing the activity of Ni-based catalysts, little progress has been made on understanding the role of iron ions in increasing the photocatalytic activity of $Ni_3(NO_3)_2(OH)_4$. Inspired by that idea, we prepared Fe doped $Ni_3(NO_3)_2(OH)_4$ and investigated iron ions incorporation on the catalytic activity of a brucite-structured $Ni_3(NO_3)_2(OH)_4$. The effects of doping ions and precipitant on the phase, structures, morphology and catalytic activity of $Ni_3(NO_3)_2(OH)_4$ were studied.

EXPERIMENTAL

Ferric nitrate [$Fe(NO_3)_3·9H_2O$], nickel nitrate [$Ni(NO_3)_2·6H_2O$], urea, absolute ethanol were purchased from Sinopharm Chemical Reagent Co. Ltd. and used as received without further purification. $Fe(NO_3)_3·9H_2O$, $Ni(NO_3)_2·6H_2O$ and urea were dissolved in 20 mL of deionized water to form uniform

solution. The resulting aqueous solution was transferred into a 50 mL Teflon-lined stainless steel autoclave. The autoclave was maintained at different temperatures without stirring and shaking. After synthesis, the products were washed three times with deionized water and ethanol. Table-1 shows the experimental conditions.

Photocatalytic experiments: The photocatalytic degradation of methyl orange was conducted in an XPA-7 type photochemical reactor (Xujiang electromechanical plant) equipped with a 300 W medium pressure mercury lamp (mean wavelength 365 nm). Reaction suspensions were prepared by adding the sample (20 mg) to 100 mL of methyl orange solution (40 mg/L). The suspensions were underwent ultrasonic treatment for 10 min and stirred in dark for 1 h to ensure an adsorption/desorption equilibrium. The suspension was irradiated under the UV light. Analytical samples were drawn from the suspension after various reaction times and analyzed by UV-visible spectrophotometer at 464 nm.

X-Ray powder diffraction (XRD) patterns were recorded using a D8 ADVANCE X-ray diffractometer with high-intensity CuK$_\alpha$ radiation (λ = 1.5406 Å). The scanning electron microscopy (SEM) micrographs and energy dispersive spectroscopy (EDS) spectra were recorded on a FEI-Sirion 200 field emission scanning electron microscope. Fourier transform infrared (FTIR) spectroscopy was obtained on a Thermo Nicolet 5700. The concentration of Fe and Ni ions were analyzed on an induced coupled plasma atomic emission spectrometer (PE Optima 2100DV ICP-AES).

RESULTS AND DISCUSSION

XRD patterns were used to confirm the phase of samples. Without adding Fe^{3+}, samples show a well-crystallized $Ni_3(NO_3)_2(OH)_4$ phase (Fig.1a1-1a4, JCPDS file No. 22-0752). The intensity of (001) peak increased gradually with more urea. But when the concentration of urea increased to 0.5 M, the intensity of diffraction peaks for $Ni_3(NO_3)_2(OH)_4$ phase dropped rapidly (Figs. 1a4 and 2b1).

After adding Fe^{3+}, all samples showed some weak diffraction peaks and could be assigned to the hexagonal $Ni_3(NO_3)_2(OH)_4$ phase (Fig. 1b, JCPDS file No. 22-0752). No diffraction peaks of iron oxide or iron hydroxide were observed. With more Fe^{3+}, the intensity of diffraction peaks increased slightly both at 140 and 180 °C (Figs.1b1-1b3, 1b6, 1b7 and 2b). We also investigated the effect of reaction time
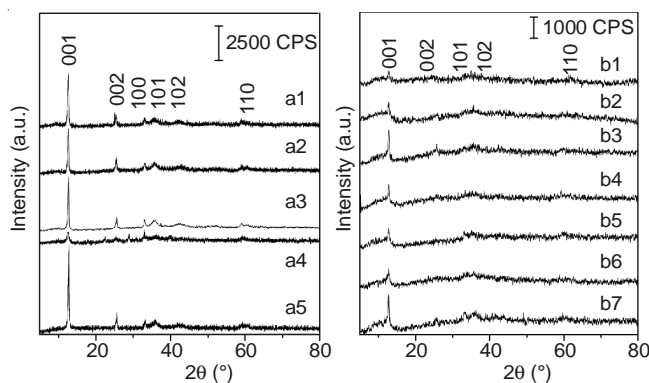

Fig. 1. XRD patterns of samples prepared (a1-a4) without Fe^{3+}, (a4) and (b) with Fe^{3+}. (a1) sample 8, (a2) sample 9, (a3) sample 10, (a4) sample 11, (a5) sample 12, (b1) sample 1, (b2) sample 2, (b3) sample 3, (b4) sample 4, (b5) sample 5, (b6) sample 6, and (b7) sample 7

and temperature on the formation of $Ni_3(NO_3)_2(OH)_4$. Under the same ratio of Fe to Ni, high reaction temperature or long reaction time led to the similar XRD patterns (Fig. 1b4-1b6). In the presence of Fe^{3+}, well-crystallized $Ni_3(NO_3)_2(OH)_4$ phase were obtained with more urea (Fig. 1b5 and 2b). Urea decomposed with an increasing temperature, which could gradually release OH^- and NH_4^+. Ni_2^+ reacted with OH^- and NO_3^- to form $Ni_3(NO_3)_2(OH)_4$. Thus, urea favors the growth of $Ni_3(NO_3)_2(OH)_4$. However, more OH^- could resist the reaction among Ni_2^+, OH^- and NO_3^-. Therefore, the crystalline of $Ni_3(NO_3)_2(OH)_4$ increased firstly and then dropped rapidly with more urea (Fig. 2). The presence of Fe led to a different result. There was a compete reaction between Fe^{3+} ions and Ni^{2+} with OH^-. And it was easier for Fe^{3+} ions to react with OH^-. Therefore, more urea was needed to form well-crystallized $Ni_3(NO_3)_2(OH)_4$ in the presence of Fe ions (Fig.1b and 1a5).

The value of the *c* lattice parameter determined from the XRD patterns is larger than the literature value for $Ni_3(NO_3)_2(OH)_4$ (c = 0.6898 nm, JCPDS file No. 22-0752). Fig. 2a shows the plot of the c lattice parameter against the concentration of urea. It could be seen that Fe-free $Ni_3(NO_3)_2(OH)_4$ showed a larger value of c lattice parameter than Fe-doped $Ni_3(NO_3)_2(OH)_4$. The contraction of the *c* cell parameter in the presence of Fe^{3+} may be due to the substitution of smaller size of Fe^{3+} (64 pm) for Ni^{2+} (69 pm) cation.

FTIR spectra also confirmed the formation of $Ni_3(NO_3)_2(OH)_4$. A group of peaks between 990 and 1384 cm^{-1} represent the vibration of NO_3^-. Two peaks observed at 2220 and 1385 cm^{-1}

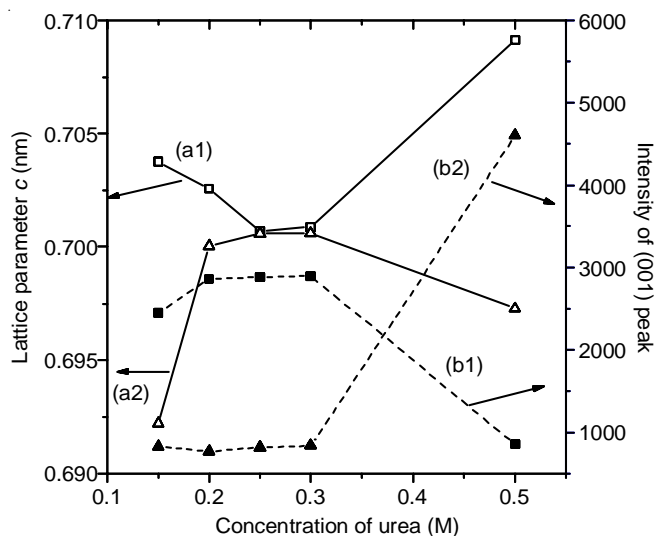| TABLE-1 EXPERIMENTAL CONDITIONS FOR SAMPLES PREPARED (0.04 M OF Ni(NO$_3$)$_2$·6H$_2$O)					
Sample no.	Fe:Ni	Urea (M)	Time (h)	Temperature (°C)	Fe:Ni (experimental results)
1	1.5:1	0.15	14	140	1.489:1
2	2:1	0.2	14	140	1.978:1
3	3:1	0.25	14	140	3.011:1
4	2:1	0.2	6	140	1.959:1
5	2:1	0.2	6	180	1.988:1
6	2:1	0.2	10	180	1.989:1
7	3:1	0.25	10	180	3.032:1
8	-	0.15	14	140	-
9	-	0.2	14	140	-
10	-	0.25	14	140	-
11	-	0.5	14	140	-
12	2:1	0.5	14	140	2.035:1

Fig. 2.   (a) Dependence of the c lattice parameter, and (b) intensity of (001) peak on urea content. (a1) and (b1) sample prepared without Fe, (a2) and (b2) sample prepared with Fe

Fig. 3.   FTIR spectra of (a) sample 12, (b) sample 11, (c) sample 3, (d) sample 10

are associated with the vibrations of -NCO, which is obtained from urea. Adding more urea resulted in stronger peaks for those vibrations of -NCO (Fig. 3a and 3b). Three peaks at 3420, 1627 and 630 cm^{-1} are associated with the vibrations of OH$^-$ [8]. Absorption at lower wavenumbers, between 740 and 480 cm^{-1}, could be attributed to vibrational modes associated to the $[M^{II,III}(OH)_2]^+$ (M = Fe^{3+} or Ni^{2+})[12]. The presence of Fe^{3+} resulted in a stronger ratio of I_{483}/I_{1384}, which may be due to the vibration of O-Fe-O.

SEM images were used to investigate the morphology and size of samples. $Ni_3(NO_3)_2(OH)_4$ spheres composed of nanosheets were prepared (Fig. 4a-4e). It has been reported that $Ni_3(NO_3)_2(OH)_4$ nanosheets were obtained through the anisotropic nucleating in ethanol by a controlled solvothermal method[8,9]. In our experiments, $Ni_3(NO_3)_2(OH)_4$ assembled

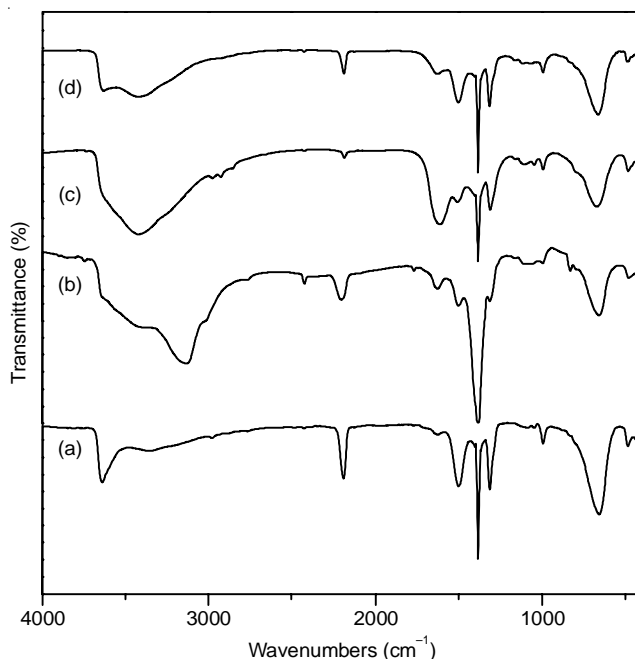spheres were also formed but using deionized water as solvent and urea as precipitant. With the increasing concentration of urea, the morphology and size of samples changed slightly. Urea has less effect on the morphology without Fe^{3+}.

After adding Fe^{3+}, the morphology of $Ni_3(NO_3)_2(OH)_4$ changed. With lower concentration of Fe^{3+}, sample 1 was spheres with porous surfaces (Fig. 5a). Increasing the amount of Fe^{3+}, samples were also spheres with some particles on the surface. But the diameters of the spheres increased (Fig. 5b and 5c). With higher temperature, some spheres with holes on the surface were observed (Fig. 5d). And no sheet like morphology was observed. However, with more urea, the
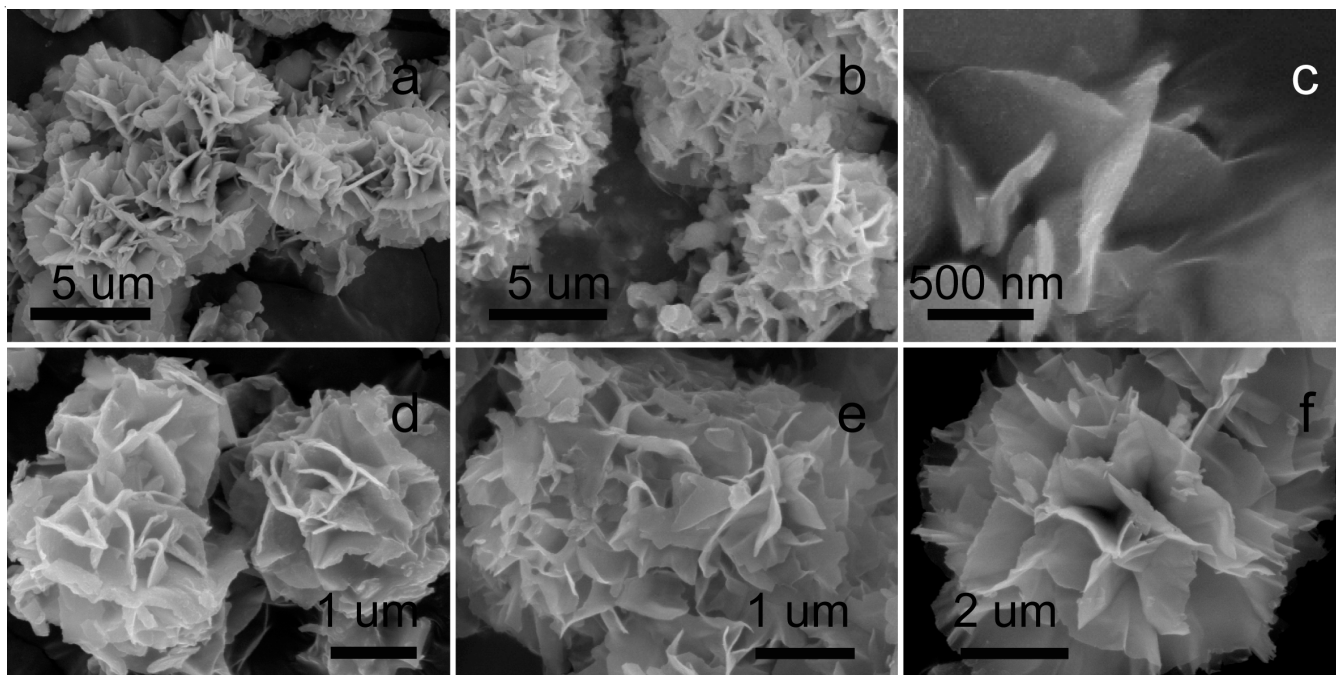

Fig. 4. SEM images of (a) sample 8, (b) and (c) sample 9, (d) sample 10, (e) sample 11, (f) sample 12
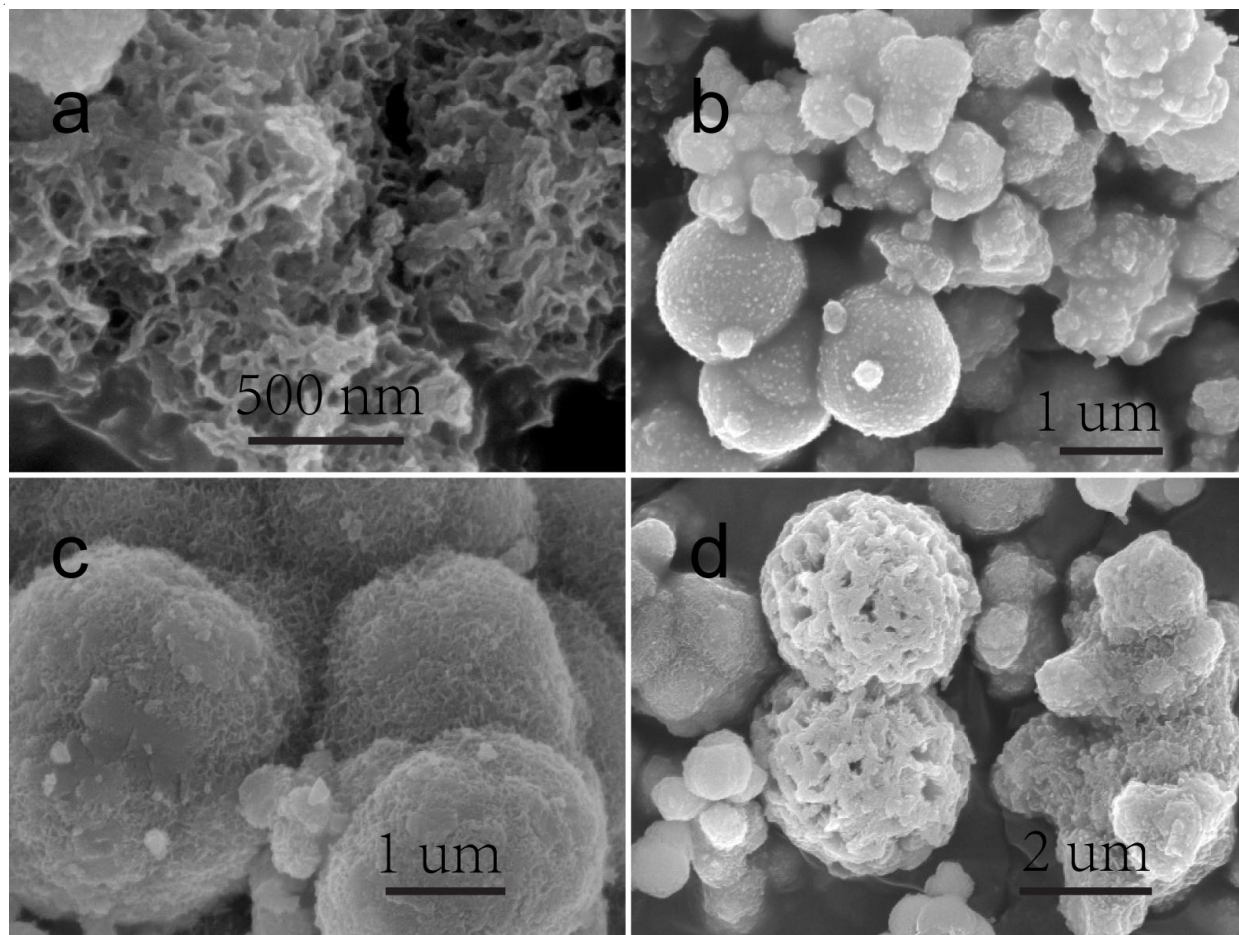
Fig. 5. SEM images of (a) sample 1, (b) sample 2, (c) sample 3, (d) sample 6

addition of Fe also led to the formation of nanosheets (Fig. 4f). EDS was used to confirm the presence of Fe. The ratio of Fe to Ni was also measured by ICP-AES (Table-1) and was similar to that of theoretical value.

It is known that when the ions in solution exceed the solubility product, it tends to form positively charged and highly anisotropic nuclei, which would result in the generation of $Ni_3(NO_3)_2(OH)_4$ nanosheets. According to XRD analysis (Fig. 1), Fe^{3+} could easily react with OH^- obtained from the decomposition of urea, which could reduce the concentration of ionic product in solution and leads to form isotropic nuclei. Therefore $Ni_3(NO_3)_2(OH)_4$ particles were obtained. Higher concentration of urea could generate more OH^- in the solution. The consumption of OH^- owing to the reaction between Fe^{3+} and OH^- has no obvious effect on the concentration of ionic product. While with more urea, the reaction between Fe^{3+} and OH^- has less effect on the concentration of ionic product. And highly anisotropic nuclei formed and $Ni_3(NO_3)_2(OH)_4$ spheres composed of nanosheets were obtained.

The photocatalytic activity of the composites in the degradation of methyl orange was investigated. Fig. 6 shows the degradation curves of methyl orange over different photocata-lysts (C_0 and C are the equilibrium concentrations of methyl orange before and after UV-irradiation, respectively). A blank experiment using sample 1 as the photocatalyst without UV-irradiation demonstrated that no methyl orange degradation occurred (Fig. 6a). The concentration of methyl orange decreased slightly under UV irradiation without any catalysts (Fig. 6b). This confirmed that methyl orange degradation is through a photocatalytic process. $Ni_3(NO_3)_2(OH)_4$ spheres composed of nanosheets without Fe^{3+} showed poor photocatalytic activity (Fig. 6c and 6d). The fast recombination rate of the photogenerated electron/hole pairs hinders the degradation of pollutions. Doping metal ions is an effective method to improve the photocatalytic properties by increasing the efficiency of charge separation and extending the energy range of photoexcitation[13]. In our experiments, the addition of Fe^{3+} led to the increase in the photocatalytic activity (Fig. 6e-6i). It is well known that the ultrathin or porous feature can further shorten the OH^- diffusion pathway, ensuring fast redox reactions[14]. Therefore, sample 1, which was sphere with holes on the surface and sample 12, which was sphere composed of sheets, showed higher photocatalytic activity. The degradation percentage of methyl orange increased rapidly with a long-time irradiation and reached about 20 % in 210 min.

Conclusion

Undoped and Fe doped $Ni_3(NO_3)_2(OH)_4$ nanosheets and particles were prepared by hydrothermal method. The effects of iron ions and urea on the preparation of $Ni_3(NO_3)_2(OH)_4$ structures were investigated. The crystalline of Fe-free $Ni_3(NO_3)_2(OH)_4$ increased first and then dropped rapidly with more urea. $Ni_3(NO_3)_2(OH)_4$ spheres composed of nanosheets were formed without Fe^{3+}. Due to the reaction between Fe^{3+}
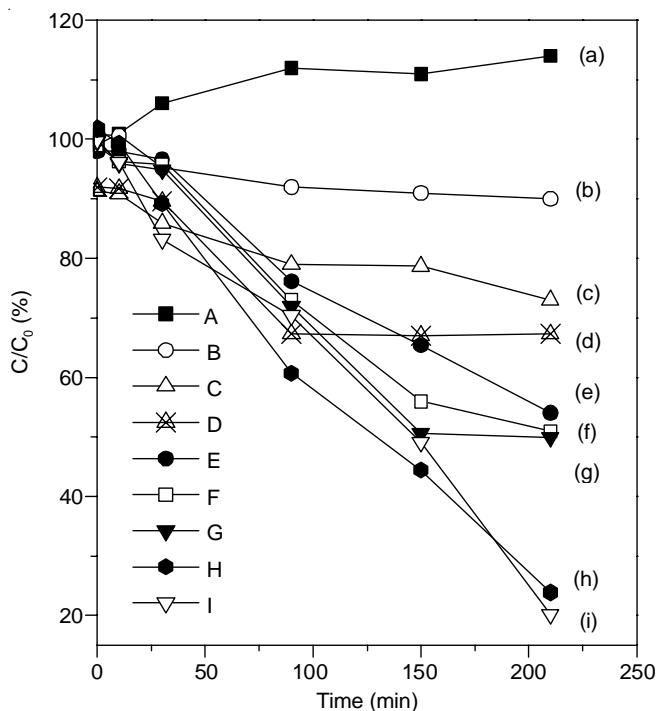
Fig. 6.   Degradation curves of methyl orange over different photocatalysts. (a) no UV, (b) no catalyst, (c) sample 8, (d) sample 11, (e) sample 3, (f) sample 2, (g) sample 6, (h) sample 1, and (i) sample 12

and urea, low concentration of urea favored the formation of Fe-doped $Ni_3(NO_3)_2(OH)_4$ particles, while high concentration preferred the formation of well-crystallized Fe-doped $Ni_3(NO_3)_2(OH)_4$ nanosheets. Doping iron ions led to a better photocatalytic activity. Fe-doped $Ni_3(NO_3)_2(OH)_4$ nanosheets and porous particles exhibited good photocatalytic activity in the degradation of methyl orange.

ACKNOWLEDGEMENTS

REFERENCES

1. M.A. Naeem, A.S. Al-Fatesh, A.E. Abasaeed and A.H. Fakeeha, *Fuel Process. Technol.*, **122**, 141 (2014).
2. M. Saeed and M. Ilyas, *Appl. Catal. B*, **129**, 247 (2013).
3. B.D. Polat, A. Abouimrane, N. Sezgin, O. Keles and K. Amine, *Electrochim. Acta*, **135**, 585 (2014).
4. Q. Du and G. Lu, *Appl. Surf. Sci.*, **305**, 235 (2014).
5. J.G. Yu, Y. Hai and B. Cheng, *J. Phys. Chem. C*, **115**, 4953 (2011).
6. M. Oshikiri, J. Ye and M. Boero, *J. Phys. Chem. C*, **118**, 12845 (2014).
7. H. Heli, N. Sattarahmady, R.D. Vais and K. Karimian, *Sens. Actuators B*, **196**, 631 (2014).
8. L.B. Kong, L. Deng, X.M. Li, M.C. Liu, Y.C. Luo and L. Kang, *Mater. Res. Bull.*, **47**, 1641 (2012).
9. Z.X. Yang, W. Zhong, C. Au, J.Y. Wang and Y.W. Du, *CrystEngComm*, **13**, 1831 (2011).
10. L. Trotochaud, S.L. Young, J.K. Ranney and S.W. Boettcher, *J. Am. Chem. Soc.*, **136**, 6744 (2014).
11. D. Tang, J. Liu, X. Wu, R. Liu, X. Han, Y. Han, H. Huang, Y. Liu and Z. Kang, *ACS Appl. Mater. Interfaces*, **6**, 7918 (2014).
12. G. Abellan, E. Coronado, C. Martí-Gastaldo, J. Waerenborgh and A. Ribera, *Inorg. Chem.*, **52**, 10147 (2013).
13. M.R. Hoffmann, S.T. Martin, W.Y. Choi and D.W. Bahnemann, *Chem. Rev.*, **95**, 69 (1995).
14. J. Liu, C. Cheng, W. Zhou, H. Li and H.J. Fan, *Chem. Commun.*, **47**, 3436 (2011).